CGC/saturation approach: Soft interaction at the LHC energies

E. Gotsman [a,*], E. Levin [a,b], I. Potashnikova [b]

[a] *Department of Particle Physics, School of Physics and Astronomy, Raymond and Beverly Sackler Faculty of Exact Science, Tel Aviv University, Tel Aviv, 69978, Israel*
[b] *Departemento de Física, Universidad Técnica Federico Santa María, and Centro Científico-Tecnológico de Valparaíso, Avda. Espana 1680, Casilla 110-V, Valparaíso, Chile*

A R T I C L E   I N F O

A B S T R A C T

In this paper we demonstrate that our model which is based on the CGC/saturation approach, is able to describe the soft interaction collisions including the new TOTEM preliminary data at 13 TeV. We believe that this strengthens the argument that the CGC/saturation approach is the only viable candidate for an effective theory for high energy QCD.

© 2018 The Author(s). Published by Elsevier B.V. This is an open access article under the CC BY license (http://creativecommons.org/licenses/by/4.0/). Funded by SCOAP³.

1. Introduction

In our recent paper [1] we have constructed a model, which allows us to discuss soft and hard processes on the same footing, it is based on the CGC/saturation approach (see Ref. [2] for a review) and on our previous attempts to build such a model [3–10].

In the model which we proposed in Ref. [1], we successfully describe the DIS data from HERA, the total, inelastic, elastic and diffractive cross sections, the t-dependence of these cross sections, as well as the inclusive production and rapidity and angular correlations in a wide range of energies, including that of the LHC.

Since the main feature, that we discuss in Ref. [1], are the angular correlations, our progress in describing the soft interaction data went unnoticed. The representatives of the TOTEM collaboration, reporting on their new preliminary results for energies W = 2.76 TeV [39] and W = 13 TeV [11], neglected to mention our model as one that provides a good description of their data (see Ref. [11]).

The goal of this letter is to draw the attention of the high energy community that our approach is successful in describing the entire set of data for high energy soft scattering, including the new experimental data from the LHC.

2. The model: theoretical input from the CGC/saturation approach

Our model incorporates two ingredients: the achievements of the CGC/saturation approach and the pure phenomenological treatment of the long distance non-perturbative physics, necessary, due to the lack of the theoretical understanding of confinement of quark and gluons.

For completeness of presentation we initially include a review of our approach, more details of which can be found in [1].

For the effective theory for QCD at high energies we have two different formulations: the CGC/saturation approach [12–15], and the BFKL Pomeron calculus [16–29]. In Ref. [28] it was shown, that these two approaches are equivalent for

$$Y \leq \frac{2}{\Delta_{\text{BFKL}}} \ln\left(\frac{1}{\Delta_{\text{BFKL}}^2}\right) \tag{1}$$

where Δ_{BFKL} denotes the intercept of the BFKL Pomeron. In our model $\Delta_{\text{BFKL}} \approx 0.2 - 0.25$ leading to $Y_{max} = 20 - 30$, which covers all collider energies.

Bearing this equivalence in mind, in constructing our model we rely on the BFKL Pomeron calculus, as the relation to diffractive physics and soft processes, is more transparent in this approach.

In the framework of the BFKL Pomeron calculus we need to solve two principle problems: to find the resulting (dressed) Pomeron Green function and to specify the interaction of the
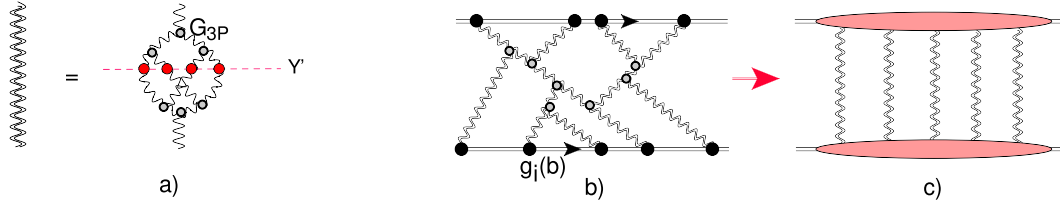

Fig. 1. Fig. 1-a shows the set of diagrams in the BFKL Pomeron calculus that produce the resulting (dressed) Green function of the Pomeron in the framework of high energy QCD. The red blobs denote the amplitude for the dipole–dipole interaction at low energy In Fig. 1-b the net diagrams, which include the interaction of the BFKL Pomerons with colliding hadrons, are shown. The sum of the diagrams after integration over positions of G_{3P} in rapidity, reduces to Fig. 1-c. The single wavy lines denote the BFKL Pomerons, while the double wavy lines describe the dressed Pomerons. (For interpretation of the colours in the figure(s), the reader is referred to the web version of this article.)

Pomeron with the hadrons. The first problem should be solved in the effective theory for high energy QCD, and the CGC/saturation approach is the only candidate for such a theory. The second problem involves a phenomenological treatment, which in our model is based on new small parameters that we determined in our fit to the experimental data.

The resulting (dressed) BFKL Pomeron Green function in CGC/saturation approach can be calculated using t-channel unitarity constraints:

$$
\begin{aligned}
&G_P^{\text{dressed}}(Y, r, R; b) \\
&= \int \prod_{i=1} d^2 r_i\, d^2 b_i\, d^2 r_i'\, d^2 b_i'\, N\left(Y - Y', r, \{r_i, b - b_i\}\right) \\
&\quad \times \boxed{A_{\text{dipole–dipole}}^{BA}\left(r_i, r_i', b_i - b_i'\right)}\, N\left(Y', R, \{r_i', b_i'\}\right)
\end{aligned}
\tag{2}
$$

where $N\left(Y - Y', r, \{r_i, b - b_i\}\right)$ denotes the amplitude for the production in the t-channel of the set of dipoles with $Y = Y'$ and with the size r_i, at impact parameters b_i. $A_{\text{dipole–dipole}}^{BA}$ denotes the dipole–dipole scattering amplitude in the Born approximation of perturbative QCD, which are indicated by red circles in Fig. 1-a. In addition, in Ref. [28] it is shown that for such Y, we can safely use the Mueller–Patel–Salam–Iancu (MPSI) approach [30]. In this approximation we can use the parton cascade of the Balitsky–Kovchegov [14] equation to find amplitudes $N\left(Y - Y', r, \{r_i, b - b_i\}\right)$ and $N\left(Y', R, \{r_i', b_i'\}\right)$, which can be viewed as a sum of the BFKL Pomeron 'fan' diagrams (see Fig. 1-a for examples of such diagrams). Generally speaking, this amplitude can be written as $N\left(Y - Y', r, \{r_i, b_i\}\right) = N^{\text{BK}}\left(Y - Y', r, \{r_i, b_i\}\right)$ (see Fig. 1-c) with

$$
\begin{aligned}
&N^{\text{BK}}\left(Y - Y', r, \{r_i, b_i\}\right) \\
&= \sum_{n=1}^{\infty} (-1)^{n+1}\, \widetilde{C}_n(r) \prod_{i=1}^{n} G_P\left(Y - Y'; r, r_i, b_i\right) \\
&= \sum_{n=1}^{\infty} (-1)^{n+1}\, \widetilde{C}_n(r) \prod_{i=1}^{n} G_P\left(z - z_i\right)
\end{aligned}
\tag{3}
$$

G_P denotes the Green function of the BFKL Pomeron. In the last equation we used the fact that in the saturation region this Green function displays geometric scaling behaviour, and it only depends on one variable: $z_i = \ln\left(Q_s^2(Y') r_i^2\right)$, where $Q_s(Y')$, is the saturation scale, in the vicinity of the saturation scale [31]

$$
G_P(z_i) = \phi_0 \left(r_i^2\, Q_s^2(Y, b_i)\right)^{1 - \gamma_{cr}} \quad \text{with} \quad \gamma_{cr} = 0.37 \tag{4}
$$

We wish to stress that this form for the Green function produces screening corrections which increase with increasing energy, and are in accord with the behaviour of the high energy LHC results.

In Ref. [29], it was shown that, the solution to the non-linear BK equation has the following general form

$$
N\left(G_P(\phi_0), z\right) = \sum_{n=1}^{\infty} (-1)^{n+1} C_n(\phi_0)\, G_P^n(z). \tag{5}
$$

Comparing Eq. (3) with Eq. (5) we see

$$
\widetilde{C}_n(r) = C_n(\phi_0). \tag{6}
$$

Hence, $\widetilde{C}_n(r)$ does not depend on r, but is a function of the BFKL Pomeron at $\tau = r^2 Q_s^2 = 1$. These coefficients are independent of r, and so provide the geometric scaling behaviour, which is a general feature of the CGC/saturation approach [35]. Coefficients C_n can be determined from the solution to the Balitsky–Kovchegov equation [14], in the saturation region. The numerical solution for the simplified BFKL kernel, in which only the leading twist contribution was taken into account, is given in Ref. [29]:

$$
N^{\text{BK}}(G_P(z)) = a\left(1 - \exp(-G_P(z))\right) + (1 - a) \frac{G_P(z)}{1 + G_P(z)}, \tag{7}
$$

with $a = 0.65$. Eq. (7) is a convenient parameterization of the numerical solution, having an accuracy of better than 5%. Having determined C_n from the numerical parameterization of Eq. (7), we can calculate the Green function of the dressed BFKL Pomeron using Eq. (2), and the property of the BFKL Pomeron exchange:

$$
\begin{aligned}
&\frac{\alpha_S^2}{4\pi}\, G_P(Y - 0, r, R; b) \\
&= \int d^2 r'\, d^2 b'\, d^2 r''\, d^2 b''\, G_P\left(Y - Y', r, r', b - b'\right) \\
&\quad \times G_P\left(Y' r'', R, b''\right) A_{\text{dipole–dipole}}^{BA}\left(r', r'', b'' - b'\right)
\end{aligned}
\tag{8}
$$

Carrying out the integrations in Eq. (2), we obtain the Green function of the dressed Pomeron in the following form:

$$
\begin{aligned}
&G^{\text{dressed}}(G_P(z)) \\
&= a^2\left(1 - \exp(-G_P(z))\right) + 2a(1 - a) \frac{G_P(z)}{1 + G_P(z)} \\
&\quad + (1 - a)^2 \widetilde{G}(G_P(z))
\end{aligned}
\tag{9}
$$

with $\widetilde{G}(T) = 1 - \frac{1}{T} \exp\left(\frac{1}{T}\right) \Gamma\left(0, \frac{1}{T}\right)$, where $\Gamma(s, z)$ is the upper incomplete gamma function (see Ref. [32] formula **8.35**). $G_P(z)$ denotes the BFKL Pomeron in the vicinity of the saturation scale (see Eq. (4)).

The Green function of Eq. (9) depends on the size of the dipoles. In our analysis of the soft interaction we fixed $r = 1/m$, m being a fitting parameter. Having the dressed Pomeron Green function, we can check quantitatively how well conventional wisdom
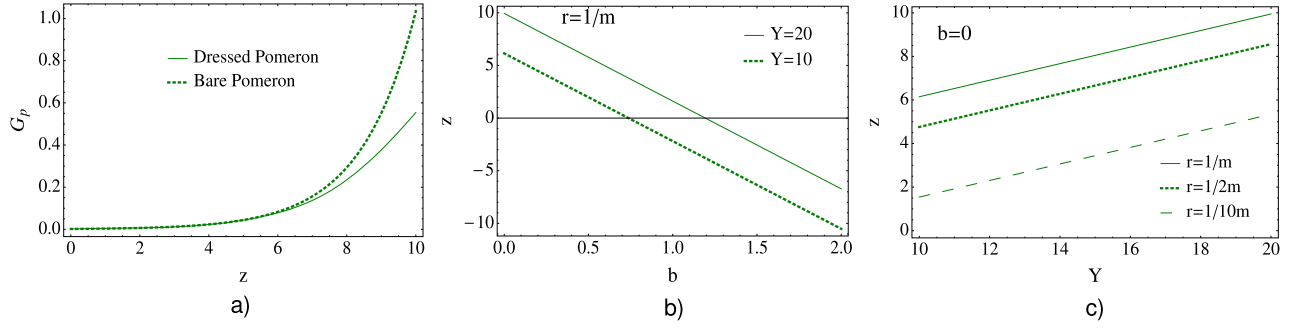
Fig. 2. The dependance of the dressed and bare Pomeron Green functions versus z (Fig. 2-a). Fig. 2-b and Fig. 2-c show the values of z in our model with the parameters of Table 1.

Table 1
Fitted parameters of the model. Fit I: parameters for the soft interaction at high energy are taken from Ref. [4]. The additional parameters for DIS were found by fitting to the F_2 structure function [1]. Fit II: joint fit to the soft interaction data at high energy and the DIS data. The values of χ^2/d.o.f. were calculated for the published data points at energies W = 0.546, 1.8, 7 an 8 TeV shown in Fig. 3.

Model	λ	ϕ_0 (GeV^{-2})	g_1 (GeV^{-1})	g_2 (GeV^{-1})	m (GeV)	m_1 (GeV)	m_2 (GeV)	β	χ^2/d.o.f.
I (soft int.)	0.38	0.0019	110.2	11.2	5.25	0.92	1.9	0.58	1.02
II (soft + DIS)	0.38	0.0022	96.9	20.96	5.25	0.86	1.76	0.66	1.28

works, i.e. that Pomeron loops only contribute at energies higher, than the experimentally accessible ones. Fig. 2 illustrates the comparison Eq. (9) and Eq. (4) for single Pomeron exchange. One can see that, indeed, at small values of z, we can neglect the Pomeron loops contribution (see Fig. 2-a). However, for $z \geq 6$ they differ, and at $z = 10$, $G_P \approx 0.5 \, G_P^{BFKL}$. In Fig. 2-b and Fig. 2-c we show the values of z using the parameters of our model. On a qualitative level we note, that the loop corrections give an essential contribution to the description of the LHC data for soft processes, at $b \leq 1$ GeV^{-1}. We wish to stress, that only by including the loop corrections and describing the experimental data, can we *a posteriori* estimate the kinematic region, in which we are justified to neglect them.

3. Phenomenology: assumptions and new small parameters

Due to the embryonic stage of theoretical understanding of the confinement of quarks and gluons, it is necessary to use pure phenomenological ideas to ameliorate two major problems in high energy scattering: the structure of hadrons, and the large impact parameter behaviour of the scattering amplitude [33]. To correct the large impact parameter behaviour, we assume that the saturation momentum has the following dependence on the impact parameter b:

$$Q_s^2 (b, Y) = Q_{0s}^2 (b, Y_0) \, e^{\lambda \, (Y - Y_0)}$$
$$\text{where} \quad Q_{0s}^2 (b, Y_0) = \left(m^2 \right)^{1 - 1/\bar{\gamma}} \, (S \, (b, m))^{1/\bar{\gamma}}$$
$$\text{with} \quad S \, (b, m) = \frac{m^2}{2\pi} e^{-mb} \tag{10}$$

In Eq. (10) $\bar{\gamma} = 1 - \gamma_{cr} = 0.63$.

We have introduced a new phenomenological parameter m to describe the large b behaviour. The Y dependence as well as r^2 dependence, can be found from the CGC/saturation approach [2], since ϕ_0 and λ can be calculated in the leading order of perturbative QCD. However, since the higher order corrections turn out to be large [34], we treat them as parameters to be fitted. m is a non-perturbative parameter, which determines the typical sizes of dipoles within the hadrons. In Table 1, we show that from the fit, $m = 5.25$ GeV, supporting our main assumption that we can apply the BFKL Pomeron calculus, based on perturbative QCD, to the

soft interaction since $m \gg \mu_{soft}$, where μ_{soft} is the scale of soft interaction, which is of the order of the mass of pion or Λ_{QCD}.

The second unsolved problem for which we need a phenomenological input, is the structure of the scattering hadrons. We use a two channel model, which allows us to calculate the diffractive production in the region of small masses. In this model, we replace the rich structure of the diffractively produced states, by a single state with the wave function ψ_D, a la Good–Walker [36]. The observed physical hadronic and diffractive states are written in the form

$$\psi_h = \alpha \, \Psi_1 + \beta \, \Psi_2; \qquad \psi_D = -\beta \, \Psi_1 + \alpha \, \Psi_2;$$
$$\text{where } \alpha^2 + \beta^2 = 1; \tag{11}$$

Functions ψ_1 and ψ_2 form a complete set of orthogonal functions $\{\psi_i\}$ which diagonalize the interaction matrix T

$$A_{i,k}^{i'k'} = < \psi_i \, \psi_k |\mathbf{T}| \psi_{i'} \, \psi_{k'} > = A_{i,k} \, \delta_{i,i'} \, \delta_{k,k'}. \tag{12}$$

The unitarity constraints take the form

$$2 \, \mathrm{Im} \, A_{i,k} (s, b) = |A_{i,k} (s, b)|^2 + G_{i,k}^{in} (s, b), \tag{13}$$

where $G_{i,k}^{in}$ denotes the contribution of all non diffractive inelastic processes, i.e. it is the summed probability for these final states to be produced in the scattering of a state i off a state k. In Eq. (13) $\sqrt{s} = W$ denotes the energy of the colliding hadrons, and b the impact parameter. A simple solution to Eq. (13) at high energies, has the eikonal form with an arbitrary opacity Ω_{ik}, where the real part of the amplitude is much smaller than the imaginary part.

$$A_{i,k}(s, b) = i \left(1 - \exp \left(-\Omega_{i,k}(s, b) \right) \right),$$
$$G_{i,k}^{in}(s, b) = 1 - \exp \left(-2 \, \Omega_{i,k}(s, b) \right). \tag{14}$$

Eq. (14) implies that $P_{i,k}^S = \exp \left(-2 \, \Omega_{i,k}(s, b) \right)$, is the probability that the initial projectiles (i, k) reach the final state interaction unchanged, regardless of the initial state re-scatterings.

The first approach is to use the eikonal approximation for Ω in which

$$\Omega_{i,k}(r_\perp, Y - Y_0, b)$$
$$= \int d^2b' \, d^2b'' \, g_i\left(\boldsymbol{b}', m_i\right) G^{\text{dressed}}\left(G_P\left(r_\perp, Y - Y_0, \boldsymbol{b}''\right)\right)$$
$$\times g_k\left(\boldsymbol{b} - \boldsymbol{b}' - \boldsymbol{b}'', m_k\right) \qquad (15)$$

where m_i denote the masses, which is introduced phenomenologically to determine the b dependence of g_i (see below). However, we do not have any reason to trust the eikonal approximation, which we found is not sufficient to fit the experimental data. We propose a more general approach, which takes into account the new small parameters, that are determined by fitting to the experimental data (see Table 1 and Fig. 1 for notation):

$$G_{3P}\Big/ g_i(b=0) \ll 1; \qquad m \gg m_1 \text{ and } m_2 \qquad (16)$$

The second equation in Eq. (16) leads to the fact that b'' in Eq. (15) is much smaller than b and b', therefore, Eq. (15) can be re-written in a simpler form

$$\Omega_{i,k}(r_\perp, Y - Y_0, b)$$
$$= \underbrace{\left(\int d^2b'' \, G^{\text{dressed}}\left(G_P\left(r_\perp, Y - Y_0, \boldsymbol{b}''\right)\right) \right)}_{\tilde{G}^{\text{dressed}}(r_\perp, Y - Y_0)}$$
$$\times \int d^2b' \, g_i\left(\boldsymbol{b}'\right) g_k\left(\boldsymbol{b} - \boldsymbol{b}'\right) \qquad (17)$$

Using the first small parameter of Eq. (16), we see that the main contribution stems from the net diagrams shown in Fig. 1-b [37]. Indeed, it turns out that the proton–proton interaction is similar to the nucleus–nucleus interaction. For a nucleus interaction $g_i \propto A^{1/3} \gg G_{3P}$ and $R_A \gg R_N$, where R_A and R_N are nucleus and nucleon radii, respectively. Eq. (16) shows the same hierarchy of the vertices and radii in proton proton scattering. As it was shown in Refs. [23,38] that the dominant contributions stem from the net diagrams of Fig. 1-b which were summed in Ref. [37].

The sum of these diagrams [4] leads to the following expression for $\Omega_{i,k}(s,b)$

$$\Omega(r, Y - Y_0; b)$$
$$= \int d^2b' \frac{g_i\left(\boldsymbol{b}'\right) g_k\left(\boldsymbol{b} - \boldsymbol{b}'\right) \tilde{G}^{\text{dressed}}(r, Y - Y_0)}{1 + G_{3P} \, \tilde{G}^{\text{dressed}}(r, Y - Y_0)\left[g_i\left(\boldsymbol{b}'\right) + g_k\left(\boldsymbol{b} - \boldsymbol{b}'\right)\right]};$$
$$g_i(b) = g_i \, S_p(b; m_i); \qquad (18)$$

where

$$S_p(b, m_i)$$
$$= \frac{1}{4\pi} m_i^3 \, b \, K_1(m_i b) \xrightarrow{\text{Fourier image}} \frac{1}{\left(1 + Q_T^2/m_i^2\right)^2}; \qquad (19)$$

$$\tilde{G}^{\text{dressed}}(r, Y - Y_0) = \int d^2b \, G^{\text{dressed}}\left(G_P\left(r, Y - Y_0, b\right)\right)$$

where $G_P(r, Y - Y_0, b)$ is given by Eq. (4).

Formula of Eq. (18) describes the net diagrams where the Green function of the BFKL Pomeron is replaced by the dressed Pomeron Green function as it is shown in Fig. 1-b. Certainly, this is not the sum of all possible Pomeron diagrams. The full set of the diagrams should also include the corrections to the triple Pomeron vertex due to Pomeron interactions. In Ref. [37] the sum of all diagrams has been calculated in the MPSI approach. We checked that the corrections that stem from the sum of the full set of the diagrams, are numerically negligible. The reason for this is the interaction at

high energy leads to a black disk with increasing radius, and we have seen from Fig. 2 that at large b, we can substitute the BFKL Pomeron for the dressed Pomeron Green function. The corrections to the MPSI approximation turns out to be small at high energies, since they decrease as $\exp\left(-\Delta_{\text{BFKL}} Y\right)$. In Ref. [28] it is shown that the MPSI approximation follows naturally from CGC/saturation approach in the limited range of rapidities given by Eq. (1).

The impact parameter dependence of $S_p(b, m_i)$ is purely phenomenological, however, Eq. (19) which has a form of the electromagnetic proton form factor, leads to the correct $(\exp(-\mu b))$ behaviour at large b [40], and has correct behaviour at large Q_T, which has been calculate in the framework of perturbative QCD [41]. We wish to draw the reader's attention to the fact that m_1 and m_2 are the two dimensional scales in a hadron, which in the framework of the constituent quark model, we assign to the size of the hadron ($R_h \propto 1/m_1$), and the size of the constituent quark ($R_Q \propto 1/m_2$). Note that $\tilde{G}^{\text{dressed}}(Y - Y_0)$ does not depend on b. In all previous formulae, the value of the triple BFKL Pomeron vertex is known: $G_{3P} = 1.29$ GeV^{-1}.

4. Physical observables

For the completeness of presentation we give here the expression of the physical observables that we used in this paper. They can be written as follows

elastic amplitude :
$$a_{el}(s,) = i\left(\alpha^4 A_{1,1} + 2\alpha^2 \beta^2 A_{1,2} + \beta^4 A_{2,2}\right); \qquad (20)$$
elastic cross section :
$$\sigma_{tot} = 2 \int d^2b \, a_{el}(s, b); \quad \sigma_{el} = \int d^2b \, |a_{el}(s, b)|^2;$$
optical theorem :
$$2\,\text{Im}\,A_{i,k}(s, t=0) = 2\int d^2b \,\text{Im}\,A_{i,k}(s, b) = \sigma_{el} + \sigma_{in} = \sigma_{tot}; \qquad (21)$$

single diffraction :
$$\sigma_{sd}^{GW} = \int d^2b \left(\alpha\beta\{-\alpha^2 A_{1,1} + (\alpha^2 - \beta^2)A_{1,2} + \beta^2 A_{2,2}\}\right)^2; \qquad (22)$$

double diffraction :
$$\sigma_{dd}^{GW} = \int d^2b \, \alpha^4 \beta^4 \left\{A_{1,1} - 2A_{1,2} + A_{2,2}\right\}^2. \qquad (23)$$

For estimates for the large mass single and double diffraction we refer our readers to Ref. [4].

5. Results of the fit

In this paper we make two fits. In the first one (fit I in Table 1) we do not change the parameters that govern the soft interactions in our model, and are shown in Table 1 and Fig. 3. The additional parameters that we need for the description of the deep inelastic data [1] were fitted using the HERA data on the deep inelastic structure function F_2. The second fit, is a joint fit to the soft strong interaction data and the DIS data. The model predictions are in accord with the data for $0.85 \leq Q^2 \leq 27$ GeV^2, while for higher values of Q^2 and of x, the model values are slightly larger than the data (see Ref. [1]).

In Table 2 we present our predictions for the soft interaction observables, in general the values obtained in the model for the soft interactions agree with the published LHC data, as well as the new preliminary TOTEM values at W = 2.7 and 13 TeV (see
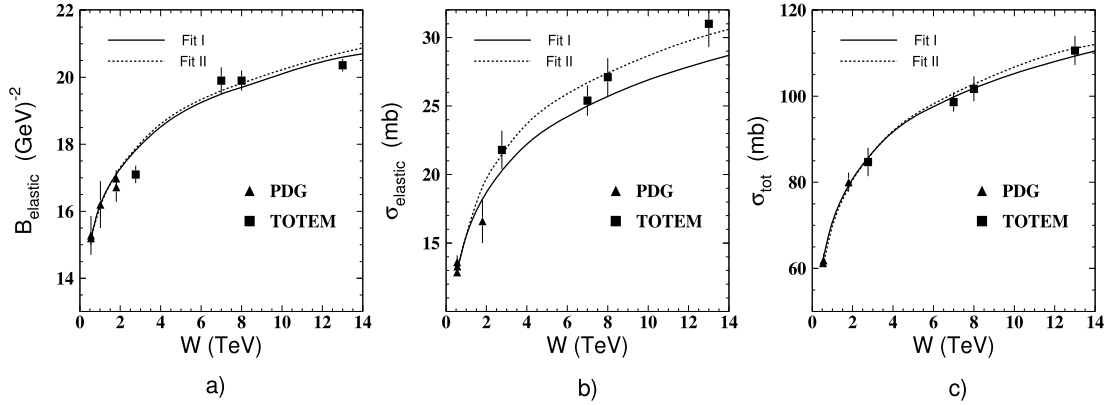
Fig. 3. The energy behaviour of σ_{tot}, σ_{el} and the slope B_{el} in our model. Fit I and fit II are explained in the text. Data are taken from Refs. [42,11,39].

Table 2
The values of cross sections and elastic slope versus energy. σ_{sd}^{smd} and σ_{dd}^{smd} denote the cross sections for diffraction dissociation in the small mass region, for single and double diffraction, which stem from the Good–Walker mechanism. While σ_{sd}^{lmd} and σ_{dd}^{lmd} denote high mass diffraction, coming from the dressed Pomeron contributions. The predictions of fit II, are shown in brackets.

W (TeV)	σ_{tot} (mb)	σ_{el} (mb)	B_{el} (GeV^{-2})	single σ_{sd}^{smd} (mb)	diffraction σ_{sd}^{lmd} (mb)	double σ_{dd}^{smd} (mb)	diffraction σ_{dd}^{lmd} (mb)
0.576	62.3(60.7)	12.9(13.1)	15.2(15.17)	5.64(4.12)	1.85(1.79)	0.7(0.39)	0.46 (0.50)
0.9	69.2(68.07)	15(15.05)	16(15.95)	6.25(4.67)	2.39(2.35)	0.77(0.46)	0.67(0.745)
1.8	79.2(78.76)	18.2(19.1)	17.1(17.12)	7.1(5.44)	3.35(3.28)	0.89(0.56)	1.17 (1.30)
2.74	85.5(85.44)	20.2(21.4)	17.8(17.86)	7.6(5.91)	4.07(4.02)	0.97(0.63)	1.62(1.79)
7	99.8(100.64)	25(26.7)	19.5(19.6)	8.7(6.96)	6.2(6.17)	1.15(0.814)	3.27(3.67)
8	101.8(102.8)	25.7(27.4)	19.7(19.82)	8.82(7.1)	6.55(6.56)	1.17(0.841)	3.63(4.05)
13	109.3(111.07)	28.3(30.2)	20.6(20.74)	9.36(7.64)	8.08(8.11)	1.27(0.942)	5.11(5.74)
14	110.5(111.97)	28.7(30.6)	20.7(20.88)	9.44(7.71)	8.34(8.42)	1.27(0.96)	5.4(6.06)
57	131.7(134.0)	36.2(38.5)	23.1(23.0)	10.85(9.15)	15.02(15.01)	1.56(1.26)	13.7(15.6)

Ref. [11,39]). We are in very good agreement with the data for σ_{tot}, σ_{el} and B_{el}.

Since the TOTEM preliminary results for energies W = 2.7 and 13 TeV, were only released after our paper [1] was published, the numbers appearing in Table 2 for these energies can be considered as predictions of our model, and are in good agreement with the TOTEM data. The one outstanding discrepancy is the value for $B_{elastic}$ at W = 2.76 TeV, where our result of 17.8 GeV^{-2} is higher than the TOTEM experimental value of 17.1 $\pm$ 0.26 GeV^{-2}, however, it is a smooth function of energy, and does not exhibit a break in the energy dependence of $B_{elastic}$, as was proposed by Csörgő [39].

Regarding σ_{sd} and σ_{dd}, a problem exists when attempting to compare with the experimental results. This is due to the difficulties of measuring diffractive events at LHC energies, the different experiments have different cuts on the values of the diffractive mass measured, making it problematic when attempting to compare the model predictions with the experimental results.

In Table 2 we show the results of the two fits, the results are close to one another, the main difference shows up only at high energies. Indeed, in fit I the cross section for single diffraction is equal to 14.9 mb, while in fit II this value is smaller (13.1 mb). The smaller value of the diffraction cross sections is closer to TOTEM and CMS data.

6. Conclusions

Fig. 3 shows that we are able to describe the experimental data on soft interaction at high energies including the LHC data. Fig. 3 shows that the screening corrections become stronger at higher energies. Our model also describes the wide range of the experimental observables: the DIS data from HERA, the total, inelastic, elastic and diffractive cross sections, the t-dependence of these cross sections as well as the inclusive production and rapidity and angular correlations in the wide range of energies including the LHC data. We believe that this fact is a strong argument in favour of the CGC/saturation approach.

Acknowledgements

References

[1] E. Gotsman, E. Levin, I. Potashnikova, Eur. Phys. J. C 77 (9) (2017) 632, arXiv: 1706.07617 [hep-ph].
[2] Yuri V. Kovchegov, Eugene Levin, Quantum Chromodynamics at High Energies, Cambridge Monographs on Particle Physics, Nuclear Physics and Cosmology, Cambridge University Press, 2012.
[3] E. Gotsman, E. Levin, U. Maor, Eur. Phys. J. C 75 (1) (2015) 18, arXiv:1408.3811 [hep-ph].
[4] E. Gotsman, E. Levin, U. Maor, Eur. Phys. J. C 75 (5) (2015) 179, arXiv:1502.05202 [hep-ph].
[5] E. Gotsman, E. Levin, U. Maor, Phys. Lett. B 746 (2015) 154, arXiv:1503.04294 [hep-ph].
[6] E. Gotsman, E. Levin, U. Maor, Eur. Phys. J. C 75 (11) (2015) 518, arXiv:1508.04236 [hep-ph].
[7] E. Gotsman, E. Levin, U. Maor, arXiv:1510.07249 [hep-ph].
[8] E. Gotsman, E. Levin, U. Maor, S. Tapia, Phys. Rev. D 93 (7) (2016) 074029, arXiv:1603.02143 [hep-ph].
[9] E. Gotsman, E. Levin, Phys. Rev. D 95 (1) (2017) 014034, arXiv:1611.01653 [hep-ph].
[10] E. Gotsman, E. Levin, Phys. Rev. D 96 (7) (2017) 074011, arXiv:1705.07406 [hep-ph].
[11] The talk at CERN, arXiv:1712.06153.

[12] L. McLerran, R. Venugopalan, Phys. Rev. D 49 (1994) 2233;
L. McLerran, R. Venugopalan, Phys. Rev. D 49 (1994) 3352;
L. McLerran, R. Venugopalan, Phys. Rev. D 50 (1994) 2225;
L. McLerran, R. Venugopalan, Phys. Rev. D 53 (1996) 458;
L. McLerran, R. Venugopalan, Phys. Rev. D 59 (1999) 09400.
[13] A.H. Mueller, Nucl. Phys. B 415 (1994) 373;
A.H. Mueller, Nucl. Phys. B 437 (1995) 107, arXiv:hep-ph/9408245.
[14] I. Balitsky, arXiv:hep-ph/9509348;
I. Balitsky, Phys. Rev. D 60 (1999) 014020, arXiv:hep-ph/9812311;
Y.V. Kovchegov, Phys. Rev. D 60 (1999) 034008, arXiv:hep-ph/9901281.
[15] J. Jalilian-Marian, A. Kovner, A. Leonidov, H. Weigert, Phys. Rev. D 59 (1999) 014014, arXiv:hep-ph/9706377;
J. Jalilian-Marian, A. Kovner, A. Leonidov, H. Weigert, Nucl. Phys. B 504 (1997) 415, arXiv:hep-ph/9701284;
J. Jalilian-Marian, A. Kovner, H. Weigert, Phys. Rev. D 59 (1999) 014015, arXiv:hep-ph/9709432;
A. Kovner, J.G. Milhano, H. Weigert, Phys. Rev. D 62 (2000) 114005, arXiv:hep-ph/0004014;
E. Iancu, A. Leonidov, L.D. McLerran, Phys. Lett. B 510 (2001) 133, arXiv:hep-ph/0102009;
E. Iancu, A. Leonidov, L.D. McLerran, Nucl. Phys. A 692 (2001) 583, arXiv:hep-ph/0011241;
E. Ferreiro, E. Iancu, A. Leonidov, L. McLerran, Nucl. Phys. A 703 (2002) 489, arXiv:hep-ph/0109115;
H. Weigert, Nucl. Phys. A 703 (2002) 823, arXiv:hep-ph/0004044.
[16] E.A. Kuraev, L.N. Lipatov, F.S. Fadin, Sov. Phys. JETP 45 (1977) 199;
Ya.Ya. Balitsky, L.N. Lipatov, Sov. J. Nucl. Phys. 28 (1978) 22.
[17] L.N. Lipatov, Phys. Rep. 286 (1997) 131;
L.N. Lipatov, Sov. Phys. JETP63 (1986) 904, and references therein.
[18] L.V. Gribov, E.M. Levin, M.G. Ryskin, Phys. Rep. 100 (1983) 1.
[19] E.M. Levin, M.G. Ryskin, Phys. Rep. 189 (1990) 267.
[20] A.H. Mueller, J. Qiu, Nucl. Phys. B 268 (1986) 427.
[21] A.H. Mueller, B. Patel, Nucl. Phys. B 425 (1994) 471.
[22] J. Bartels, M. Braun, G.P. Vacca, Eur. Phys. J. C 40 (2005) 419, arXiv:hep-ph/0412218;
J. Bartels, C. Ewerz, JHEP 9909 (1999) 026, arXiv:hep-ph/9908454;
J. Bartels, M. Wusthoff, Z. Phys. C 6 (1995) 157;
J. Bartels, Z. Phys. C 60 (1993) 471.
[23] M.A. Braun, Phys. Lett. B 632 (2006) 297, arXiv:hep-ph/0512057;
M.A. Braun, Eur. Phys. J. C 16 (2000) 337, arXiv:hep-ph/0001268;
M.A. Braun, Phys. Lett. B 483 (2000) 115, arXiv:hep-ph/0003004;
M.A. Braun, Eur. Phys. J. C 33 (2004) 113, arXiv:hep-ph/0309293;
M.A. Braun, Eur. Phys. J. C 6 (1999) 321, arXiv:hep-ph/9706373;
M.A. Braun, G.P. Vacca, Eur. Phys. J. C 6 (1999) 147, arXiv:hep-ph/9711486.
[24] Y.V. Kovchegov, E. Levin, Nucl. Phys. B 577 (2000) 221, arXiv:hep-ph/9911523.
[25] E. Levin, M. Lublinsky, Nucl. Phys. A 763 (2005) 172, arXiv:hep-ph/0501173;

E. Levin, M. Lublinsky, Phys. Lett. B 607 (2005) 131, arXiv:hep-ph/0411121;
E. Levin, M. Lublinsky, Nucl. Phys. A 730 (2004) 191, arXiv:hep-ph/0308279.
[26] E. Levin, J. Miller, A. Prygarin, Nucl. Phys. A 806 (2008) 245, arXiv:0706.2944 [hep-ph].
[27] T. Altinoluk, C. Contreras, A. Kovner, E. Levin, M. Lublinsky, A. Shulkim, Int. J. Mod. Phys. Conf. Ser. 25 (2014) 1460025;
T. Altinoluk, N. Armesto, A. Kovner, E. Levin, M. Lublinsky, J. High Energy Phys. 1408 (2014) 007.
[28] T. Altinoluk, A. Kovner, E. Levin, M. Lublinsky, J. High Energy Phys. 1404 (2014) 075, arXiv:1401.7431 [hep-ph];
T. Altinoluk, C. Contreras, A. Kovner, E. Levin, M. Lublinsky, A. Shulkin, J. High Energy Phys. 1309 (2013) 115.
[29] E. Levin, J. High Energy Phys. 1311 (2013) 039, arXiv:1308.5052 [hep-ph].
[30] A.H. Mueller, B. Patel, Nucl. Phys. B 425 (1994) 471;
A.H. Mueller, G.P. Salam, Nucl. Phys. B 475 (1996) 293, arXiv:hep-ph/9605302;
G.P. Salam, Nucl. Phys. B 461 (1996) 512;
E. Iancu, A.H. Mueller, Nucl. Phys. A 730 (2004) 460, arXiv:hep-ph/0308315;
E. Iancu, A.H. Mueller, Nucl. Phys. A 730 (2004) 494, arXiv:hep-ph/0309276.
[31] A.H. Mueller, D.N. Triantafyllopoulos, Nucl. Phys. B 640 (2002) 331; arXiv:hep-ph/0205167.
[32] I. Gradstein, I. Ryzhik, Table of Integrals, Series, and Products, fifth edition, Academic Press, London, 1994.
[33] A. Kovner, U.A. Wiedemann, Phys. Rev. D 66 (2002) 051502, arXiv:hep-ph/0112140;
A. Kovner, U.A. Wiedemann, Phys. Rev. D 66 (2002) 034031, arXiv:hep-ph/0204277;
A. Kovner, U.A. Wiedemann, Phys. Lett. B 551 (2003) 311, arXiv:hep-ph/0207335.
[34] V.A. Khoze, A.D. Martin, M.G. Ryskin, W.J. Stirling, Phys. Rev. D 70 (2004) 074013, arXiv:hep-ph/0406135;
D.N. Triantafyllopoulos, Nucl. Phys. B 648 (2003) 293, arXiv:hep-ph/0209121.
[35] E. Levin, K. Tuchin, Nucl. Phys. B 573 (2000) 833, https://doi.org/10.1016/S0550-3213(99)00825-1, arXiv:hep-ph/9908317.
[36] M.L. Good, W.D. Walker, Phys. Rev. 120 (1960) 1857.
[37] E. Gotsman, E. Levin, U. Maor, Eur. Phys. J. C 71 (2011) 1553, arXiv:1010.5323 [hep-ph].
[38] A. Kormilitzin, E. Levin, J.S. Miller, Nucl. Phys. A 859 (2011) 87, arXiv:1009.1329 [hep-ph].
[39] T. Csörgő, talk at "Low x 2017", Bisceglie, June 13–17, 2017.
[40] M. Froissart, Phys. Rev. 123 (1961) 1053;
A. Martin, Scattering Theory: Unitarity, Analyticity and Crossing, Lecture Notes in Physics, Springer-Verlag, Berlin–Heidelberg–New York, 1969.
[41] G.P. Lepage, S.J. Brodsky, Phys. Rev. Lett. 43 (1979) 545;
Phys. Rev. Lett. 43 (1979) 1625.
[42] C. Amsler, et al., Particle Data Group, Phys. Lett. B 667 (2008) 1.